GMR
The Original

EXPLORING THE MOLECULAR MECHANISMS OF EPICATECHIN FROM THE ENDOPHYTIC FUNGUS CHAETOMIUM GLOBOSUM IN RHEUMATOID ARTHRITIS USING NETWORK PHARMACOLOGY AND MOLECULAR DOCKING

Swetha R[1], Jagadeeswari. S[2], Sandhiya Viswanathan[3], B. Kirthiga[1*]

[1]Research Scholar, PG & Research Department of Microbiology, Dwaraka Doss Goverdhan Doss Vaishnav College, Chennai, Tamil Nadu, India – 600106. E mail: swethapandian.r@gmail.com
[2]Associate Professor& Head- PG & Research Department of Microbiology, Dwaraka Doss Goverdhan Doss Vaishnav College (Autonomous), Chennai, Tamil Nadu – 600106, India. Email: jagadeeswari@dgvaishnavcollege.edu.in
[3]Research Scientist, School of Biotechnology, Kalinga Institute of Industrial Technology (KIIT) Deemed to be University, Bhubaneswar - 751024, Odisha, 600013. E mail: ssandia12@gmail.com
[1*]Associate Professor, PG & Research Department of Microbiology, Dwaraka Doss Goverdhan Doss Vaishnav College, Chennai, Tamil Nadu, India – 600106. E mail: kirthiga@dgvaishnavcollege.edu.in

ABSTRACT
Endophytic fungi from medicinal plants represent valuable sources of bioactive secondary metabolites with diverse pharmacological properties. This study aimed to characterize the metabolite profile of Chaetomium globosum SK04 isolated from Drynaria quercifolia and explore its molecular mechanism in rheumatoid arthritis. The ethyl acetate extract was chromatographically fractionated, and MF5 exhibited the highest anti-inflammatory activity among the fractions, with 79.86 ± 0.03% inhibition of albumin denaturation and 77.52 ± 0.04% HRBC membrane stabilization. LC–MS/MS profiling of MF5 identified eight metabolites, among which epicatechin showed a prominent peak and was selected for further analysis. A total of 126 non-redundant potential targets of epicatechin were identified, of which 43 overlapped with rheumatoid arthritis-associated targets. PPI network analysis highlighted AKT1 as a central hub among the core targets. GO and KEGG pathway enrichment analyses revealed significant enrichment of biological processes and signalling pathways, particularly the PI3K–Akt signalling pathway. The 10 core pathways and 43 common targets were further integrated into a compound–target–pathway–disease network, in which AKT1 occupied a central position. Molecular docking showed the highest binding of epicatechin to KDR at −9.57 kcal/mol. Thus, this study provides insights into the potential molecular mechanisms of epicatechin in rheumatoid arthritis.

KEYWORDS: Chaetomium globosum; Epicatechin, Network pharmacology, Rheumatoid arthritis.

INTRODUCTION
Rheumatoid arthritis (RA) is a progressive inflammatory polyarthritis in which persistent synovial inflammation causes cartilage and bone destruction, leading to joint deformity and functional impairment (Komatsu & Takayanagi, 2022). In 2020, approximately 17.6 million people worldwide were affected by RA, with the global burden projected to reach 31.7 million by 2050, emphasizing the need for improved therapeutic approaches (Harlianto & GBD 2021 Rheumatoid Arthritis Collaborators, 2023).

RA arises from a complex interplay of genetic susceptibility, environmental factors, loss of immune tolerance, and dysregulated inflammatory responses. Rheumatoid factor and anti-citrullinated protein antibodies, together with activated T cells, B cells, macrophages, and synovial fibroblasts, contribute to persistent synovial inflammation. These events involve intracellular JAK–STAT, MAPK, PI3K–AKT, and NF-κB signalling pathways, which regulate inflammatory cytokine production, synovial proliferation, matrix degradation, and osteoclastogenesis, ultimately promoting cartilage and bone erosion (Padyukov, 2022; Ding et al., 2023).

The involvement of these signalling pathways in RA has led to the development of synthetic therapeutics targeting inflammatory mediators and signalling components. Current treatment primarily including disease-modifying antirheumatic drugs (DMARDs), such as methotrexate and other conventional synthetic DMARDs, biological and targeted synthetic DMARDs, while glucocorticoids and non-steroidal anti-inflammatory drugs (NSAIDs) for controlling inflammation and symptoms. Although these therapeutic approaches have improved disease control, prolonged treatment can cause adverse effects and treatment intolerance, while pharmacokinetic limitations such as poor solubility, permeability, bioavailability, first-pass metabolism, and nonspecific systemic distribution can affect therapeutic efficacy (Gao et al., 2024). These limitations have led to continued investigation of medicinal plants and their constituents as potential sources of anti-inflammatory and anti-rheumatic agents.

In this context, Drynaria quercifolia (L.) J. Sm. is an epiphytic medicinal pteridophyte whose rhizome has been reported to possess anti-inflammatory and anti-arthritic properties, along with diverse phytoconstituents (Jegan et al., 2025; Modak et al., 2025). Endophytic fungi residing within medicinal plants are sources of structurally diverse secondary metabolites, and their association with host plants influence secondary-metabolite biosynthesis (Alam et al., 2021). In our previous

study, the endophytic fungus Chaetomium globosum SK04 isolated from D. quercifolia exhibited anti-inflammatory and antioxidant activities (Swetha et al., 2026). However, the metabolites underlying these activities and their relevance to RA-associated molecular targets remain insufficiently characterized. The present study aimed to characterize the metabolites of C. globosum SK04 by LC–MS/MS and explore the potential molecular mechanism against RA using network pharmacolog and molecular docking.

MATERIALS AND METHODS

Production of Secondary metabolites

The endophytic fungus Chaetomium globosum SK04 used in the present study was isolated according to our previously reported study (Swetha et al., 2026). The isolate was cultivated in an optimized production medium [potato extract powder (equivalent to 100 g potato/L), glucose (10 g/L), yeast extract (2 g/L), and $MgSO_4 \cdot 7H_2O$ (0.4 g/L)]. The pH was adjusted to 6.5 prior to sterilization, and the culture was incubated at 25 °C for 16 days. After incubation, the culture broth was filtered to separate the mycelial mat from the culture filtrate. Both the mycelial mat and culture filtrate were extracted separately three times with ethyl acetate (EtOAc). The combined ethyl acetate extracts were concentrated using a rotary evaporator to obtain the crude extracts.

Bioactive fractionation of Secondary metabolites

The obtained crude extract was fractionated using a column packed with silica gel (SiO_2, 60–120 mesh) as the stationary phase, with a solvent system comprising toluene, ethyl acetate, and formic acid in a 4:5:1 (v/v) ratio. Twenty-four fractions were collected and analysed by thin-layer chromatography (TLC). Fractions showing similar Rf values were pooled to obtain the major fractions.

In vitro Screening of fractions for Anti inflammatory property

The major fractions were screened for in vitro anti-inflammatory activity using the HRBC membrane stabilization assay and albumin denaturation assay according to the previously reported methodology (Swetha et al., 2026).

Metabolite profiling- LC-MS/MS

The bioactive fraction was dissolved in methanol (5 mg/mL), vortexed, centrifuged at 13,300 rpm for 10 min, and filtered through a 0.45 µm membrane filter prior to LC–MS/MS analysis. Chromatographic separation was performed using an Agilent 1260 binary pump equipped with an autosampler, coupled to a Varian MS 500 mass spectrometer with an ion-trap analyzer. Separation was achieved on an Agilent Eclipse Plus C18 column (2.1 × 150 mm, 3.5 µm) using 0.1% formic acid in water (A) and 0.1% formic acid in acetonitrile (B) as the mobile phases. Electrospray ionization (ESI) was employed as the ionization source and operated in negative (ESI−) ionization modes. The detected precursor ions were subjected to MS/MS fragmentation, and the resulting product-ion spectra were compared with previously reported database for tentative metabolite identification.

Network Pharmacology analysis

Target Gene Prediction

The SwissTargetPrediction tool (https://www.swisstargetprediction.ch/) (Daina & Zoete, 2024) and PharmMapper platform (https://www.lilab-ecust.cn/pharmmapper/) were used to predict the potential protein targets of the selected compound (Liu et al., 2010). The canonical SMILES of the compound was submitted to SwissTargetPrediction, whereas its SDF structure was uploaded to the PharmMapper server. Homo sapiens was selected as the target species, and the predicted protein targets were standardized to gene symbols. Targets with a SwissTargetPrediction probability score ≥0.6 and a PharmMapper Norm Fit score ≥0.6048 were retained for further analysis. Meanwhile, rheumatoid arthritis-associated genes were retrieved from the GeneCards database (https://www.genecards.org/) using the keyword "rheumatoid arthritis," and genes with a relevance score >0.6 were selected. The predicted compound targets and rheumatoid arthritis-associated genes were compared, and their overlapping targets were identified using a Venn diagram generated with Venny 2.1 (https://bioinfogp.cnb.csic.es/tools/venny/)

Protein–Protein Interaction (PPI) Network Analysis

A protein–protein interaction (PPI) network was generated from the common targets using the STRING database (https://string-db.org/) (Szklarczyk et al., 2023)..Homo sapiens was selected as the organism, and interactions with a confidence score ≥0.4 were retained for network analysis. Disconnected nodes were removed. The resulting PPI network was visualized using Cytoscape (version 3.10.4), where nodes represented the common target proteins and edges represented protein–protein interactions. The MCODE plugin was used to identify densely connected protein clusters, while cytoHubba was employed to determine the hub genes based on network topology.

GO Enrichment and KEGG Pathway Analysis

The common target genes were subjected to GO functional and KEGG pathway enrichment analysis using the Metascape database (http://www.metascape.org/) (Zhou et al., 2019). Homo sapiens was selected as the species, and a P-value cutoff of 0.01 with a minimum overlap of 3 was applied. GO enrichment analysis was performed for biological process (BP), cellular component (CC), and molecular function (MF), along with KEGG pathway analysis. The significantly enriched GO terms and KEGG pathways were ranked according to gene count in descending order and used for subsequent visualization. The resulting enrichment data were further analyzed and visualized using Bioinformatics software (https://www.bioinformatics.com.cn/en).

Drug–Compound-Target–Pathway-Disease (D-C-T-P-D) Network Construction

The Drug–Compound–Target–Pathway–Disease (D-C-T-P-D) network was constructed using Cytoscape software (version 3.10.4) (Piñero et al., 2021) by integrating the selected compounds, intersecting target genes, enriched KEGG pathways, and rheumatoid arthritis (RA). Network topology was evaluated based on node degree.

In Silico Binding Affinity Assessment of Target Proteins

Preparation of Target proteins

The crystal structures of AKT1 (PDB ID: 3CQW), EGFR (PDB ID: 1M17), BCL2 (PDB ID: 4LVT), MMP9 (PDB ID: 2OW0), KDR (PDB ID: 3VO3) and MMP3 (PDB ID: 1G4K) were retrieved from the RCSB Protein Data Bank (https://www.rcsb.org/). The proteins were prepared by removing water molecules and co-crystallized ligands prior to docking.

Ligand Pre-processing

Ligand structures in SDF format were converted to PDB format using Open Babel and subsequently prepared for docking.

Molecular Docking simulation

AutoDock 4.2 was used to evaluate the binding affinity between the selected bioactive compounds and selected target proteins associated with rheumatoid arthritis (Kumar Gandham et al., 2024). Docking simulations were performed within the predefined active sites of the target proteins, as summarized in Table 1. Several docking conformations were generated for each protein–ligand complex and evaluated based on their binding energies (kcal/mol). The minimum energy conformation was selected for subsequent protein–ligand interaction analysis using Discovery Studio Visualizer. The binding affinity values obtained from molecular docking were visualized as a heatmap using SRplot (https://www.bioinformatics.com.cn/en).

Table 1. Protein Targets and site specific docking region

Protein	PDB ID	Resolution (Å)	Site-specific docking region
AKT1	3CQW	2.00	ATP-binding pocket
EGFR	1M17	2.60	ATP-binding pocket
BCL2	4LVT	2.10	BH3-binding groove
MMP9	2OW0	2.00	Catalytic Zn^{2+} active site
KDR	3VO3	1.70	ATP-binding pocket
MMP3	1G4K	2.00	Catalytic Zn^{2+} active site

RESULTS

Bioactive fractionation of Secondary metabolites

Twenty-four minor fractions (mf) obtained from column chromatography were pooled based on similar Rf values to yield major fractions (MF). The pooled fractions were evaluated for anti-inflammatory activity (Table 2). Among the tested fractions, MF5 exhibited the highest activity, with albumin denaturation inhibition of 79.86 ± 0.03% and HRBC membrane stabilization of 77.52 ± 0.04%. MF9 also showed notable activity, whereas MF1 and MF6 exhibited lower inhibition. MF5 was identified as the active fraction and selected for further characterization.

Table 2. In Vitro Anti-inflammatory Activity of the Major Fractions

Major Fraction (MF)	Albumin Denaturation Inhibition (%)	HRBC Membrane Stabilization (%)
MF1	0	0
MF2	32.48 ± 0.04	29.86 ± 0.03
MF3	26.73 ± 0.03	23.51 ± 0.04
MF4	41.95 ± 0.04	38.72 ± 0.03
MF5	79.86 ± 0.03	77.52 ± 0.04
MF6	0	0
MF7	52.38 ± 0.04	48.95 ± 0.04
MF8	21.74 ± 0.03	19.46 ± 0.03
MF9	66.81 ± 0.04	59.27 ± 0.03
MF10	39.54 ± 0.03	36.18 ± 0.04
MF11	48.93 ± 0.04	45.74 ± 0.03

Metabolite profiling- LC-MS/MS

The active MF5 fraction was subjected to LC–MS/MS analysis in the negative ion mode. Several chromatographic peaks were observed, and eight compounds were tentatively identified based on their retention times, precursor m/z values, and characteristic MS/MS fragmentation patterns (Table 3; Fig. 1). The identified metabolites comprised phenolic acids, a coumarin, an alkaloid, flavonoids and a flavonoid glycoside. Epicatechin was identified as a major metabolite based on its relatively high chromatographic abundance in the LC–MS profile and selected for further investigation. The corresponding precursor ion of epicatechin was detected at m/z 289.0722 $[M–H]^-$, with characteristic product ions at m/z 245.1, 205.1, and 179.1.

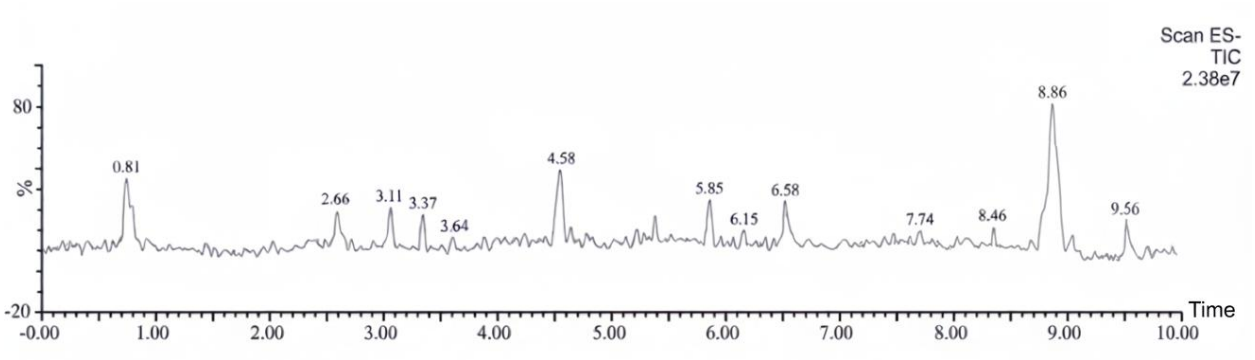


Figure 1. LC–MS/MS Chromatogram of the Active MF5 Fraction in Negative Ion Mode

Table 3. Metabolite Profiling of the Active MF5 Fraction of SK04

No.	Compound	RT (min)	Precursor ion m/z $[M–H]^-$
1	Vanillic acid	2.66	167.023
2	Umbelliferone	3.11	161.0246
3	p-Coumaric acid	3.37	163.0400
4	4-Hydroxy-3-methoxycinnamic acid	4.58	193.0506
5	Coclaurine	5.85	284.128
6	Kaempferol	6.15	285.0405
7	Syringetin-3-O-galactoside	6.58	507.123
8	Epicatechin	8.86	289.0722

Network Pharmacology analysis

Target Gene Prediction

The potential protein targets of epicatechin were predicted using PharmMapper and SwissTargetPrediction. After removal of duplicate entries, 126 non-redundant targets were obtained. A total of 930 rheumatoid arthritis (RA)-associated targets were identified from the GeneCards database based on a relevance score >0.6. The overlap between epicatechin-associated targets and RA-associated targets identified 43 common targets (Figure 2). These common targets were considered potential targets involved in the action of epicatechin against RA (Table 4).

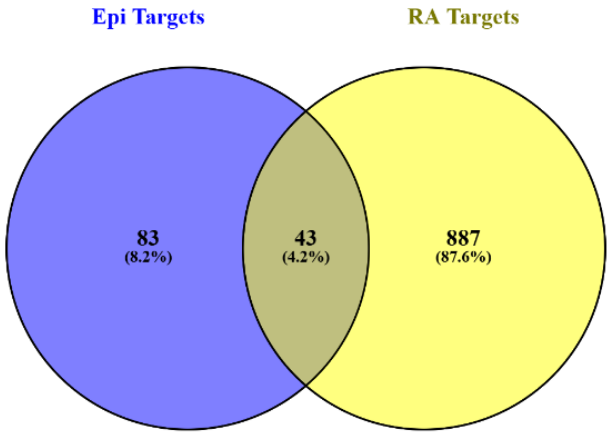


Fig 2. Venn diagram of potential Targets

* Epi represents Epicatechin, RA represents rheumatoid arthritis

Table 4. The 43 potential targets of epicatechin against rheumatoid arthritis

No.	Target	Symbol	No.	Target	Symbol
1	Carbonic anhydrase 2	CA2	23	Phosphatidylinositol 3-kinase catalytic subunit gamma	PIK3CG
2	Sclerostin	SOST	24	Glutathione reductase	GSR
3	Prostaglandin G/H synthase 1	PTGS1	25	Stromelysin-1	MMP3
4	ATP-dependent translocase ABCB1	ABCB1	26	Complement factor B	CFB
5	Apoptosis regulator Bcl-2	BCL2	27	Sex hormone-binding globulin	SHBG
6	Matrix metalloproteinase-9	MMP9	28	Mitogen-activated protein kinase 14	MAPK14
7	72 kDa type IV collagenase	MMP2	29	Disintegrin and metalloproteinase domain-containing protein 17	ADAM17
8	Vascular endothelial growth factor receptor 2	KDR	30	Collagenase 3	MMP13
9	Fibroblast growth factor receptor 1	FGFR1	31	B-Raf proto-oncogene serine/threonine-protein kinase	BRAF
10	Mast/stem cell growth factor receptor	KIT	32	Neutrophil collagenase	MMP8
11	Phosphatidylinositol 4,5-bisphosphate 3-kinase catalytic subunit alpha	PIK3CA	33	Cyclin-dependent kinase 6	CDK6
12	Telomerase reverse transcriptase	TERT	34	RAC-alpha serine/threonine-protein kinase	AKT1
13	Estrogen receptor 1	ESR1	35	Purine-nucleoside phosphorylase	PNP
14	Glycogen synthase kinase-3 beta	GSK3B	36	Dihydrofolate reductase	DHFR
15	Transthyretin	TTR	37	Macrophage metalloelastase	MMP12
16	A disintegrin and metalloproteinase with thrombospondin motifs 4	ADAMTS4	38	Dual specificity protein phosphatase 6	DUSP6
17	Placenta growth factor	PGF	39	Cathepsin K	CTSK
18	Vascular endothelial growth factor A	VEGFA	40	Macrophage migration inhibitory factor	MIF
19	Prostaglandin E synthase	PTGES	41	Epidermal growth factor receptor	EGFR
20	Aromatase	CYP19A1	42	Tyrosine-protein kinase JAK3	JAK3
21	Interstitial collagenase	MMP1	43	Thymidylate synthase	TYMS
22	Mitogen-activated protein kinase 8	MAPK8			

Protein–Protein Interaction (PPI) Network Analysis

The intersection targets were imported into the STRING database to construct a protein–protein interaction (PPI) network (Figure 3A). The resulting network comprised 42 nodes and 256 edges. The PPI network was subsequently visualized and analyzed using Cytoscape. The targets were ranked according to their degree values, and the top 30 highly connected targets were depicted in Figure 3B. MCODE analysis identified two densely interconnected clusters, with the highest-scoring cluster (Cluster 1) comprising 14 nodes and 128 edges, with an MCODE score of 9.846 (Figure 4A). The top 10 hub targets were identified using CytoHubba based on degree values (Figure 4B).

(A) **(B)**

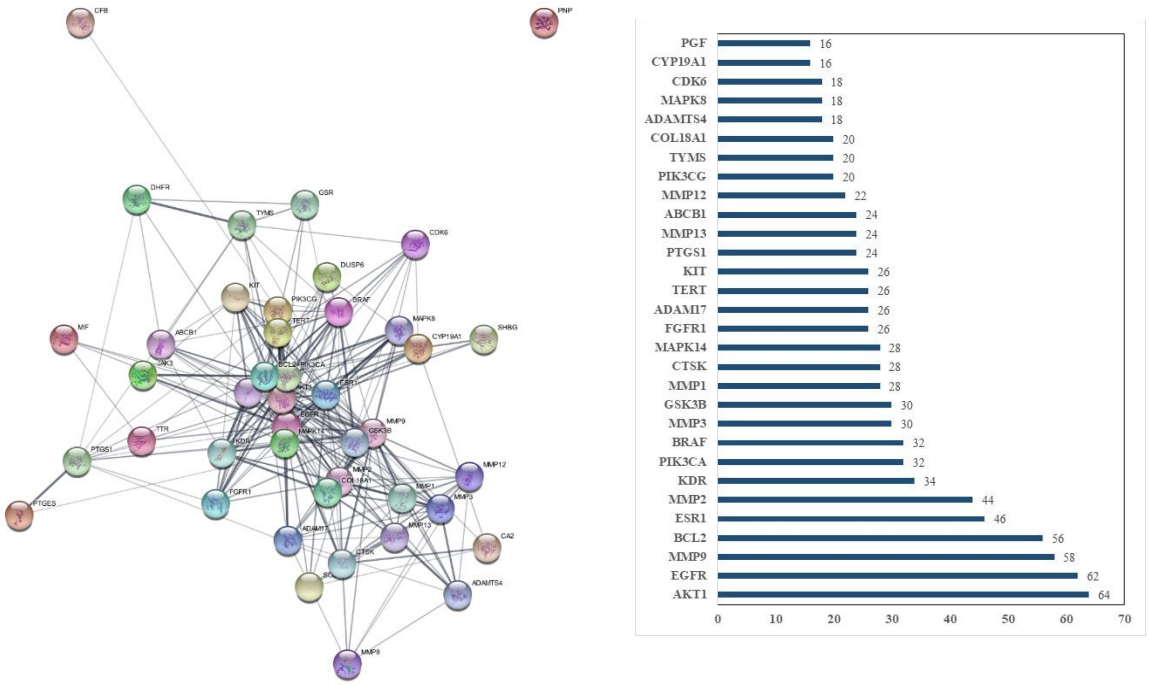
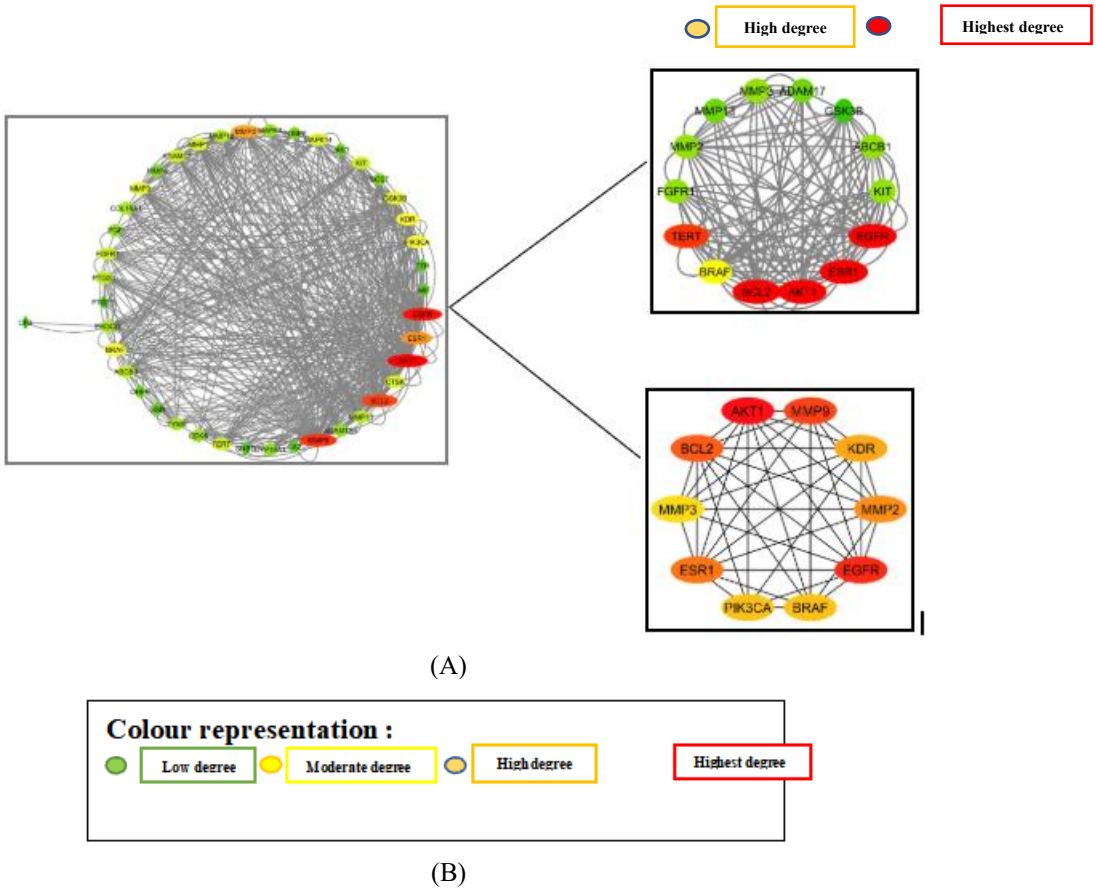


Fig. 3. (A) Protein–protein interaction (PPI) network of the shared targets constructed using the STRING database. (B) Top 30 targets ranked by the degree value.



(A)

(B)

Figure 4. MCODE and CytoHubba analysis of the PPI network. (A) Interconnected gene clusters identified by MCODE analysis and (B) Hub genes identified using CytoHubba based on degree values.

GO Enrichment and KEGG Pathway Analysis

A total of 448 significantly enriched GO terms ($p < 0.01$) were identified in the Biological Process (BP), Cellular Component (CC), and Molecular Function (MF) categories through GO enrichment analysis. The 10 most enriched terms per each category were chosen for visualization (Figure 5A). The enriched BP terms were predominantly associated with collagen and extracellular matrix remodeling, endothelial cell chemotaxis, VEGF signaling, and prostaglandin/prostanoid biosynthetic processes. Granule- and vesicle-associated components, extracellular matrix, and membrane-associated structures were the primary categories enriched in the CC category. Most of the MF category was associated with fibronectin and collagen binding, metallopeptidase activity, and protein kinase-related activities. Several pathways were

found to be significantly enriched ($p < 0.01$) through KEGG pathway enrichment analysis, including PI3K–Akt signaling, MAPK signaling, focal adhesion, Rap1 signaling, relaxin signaling, and endocrine resistance (Figure 5B). The bubble plot shows the enrichment ratio on the x-axis, the number of targets in each bubble as the size of the bubble, and the level of statistical significance by the intensity of the color. The relationships between enriched pathways and their associated targets were further illustrated using a chord diagram (Figure 5C). The identified targets were also mapped to the PI3K–Akt signaling pathway to illustrate the distribution of targets in the pathway (Figure 5D).

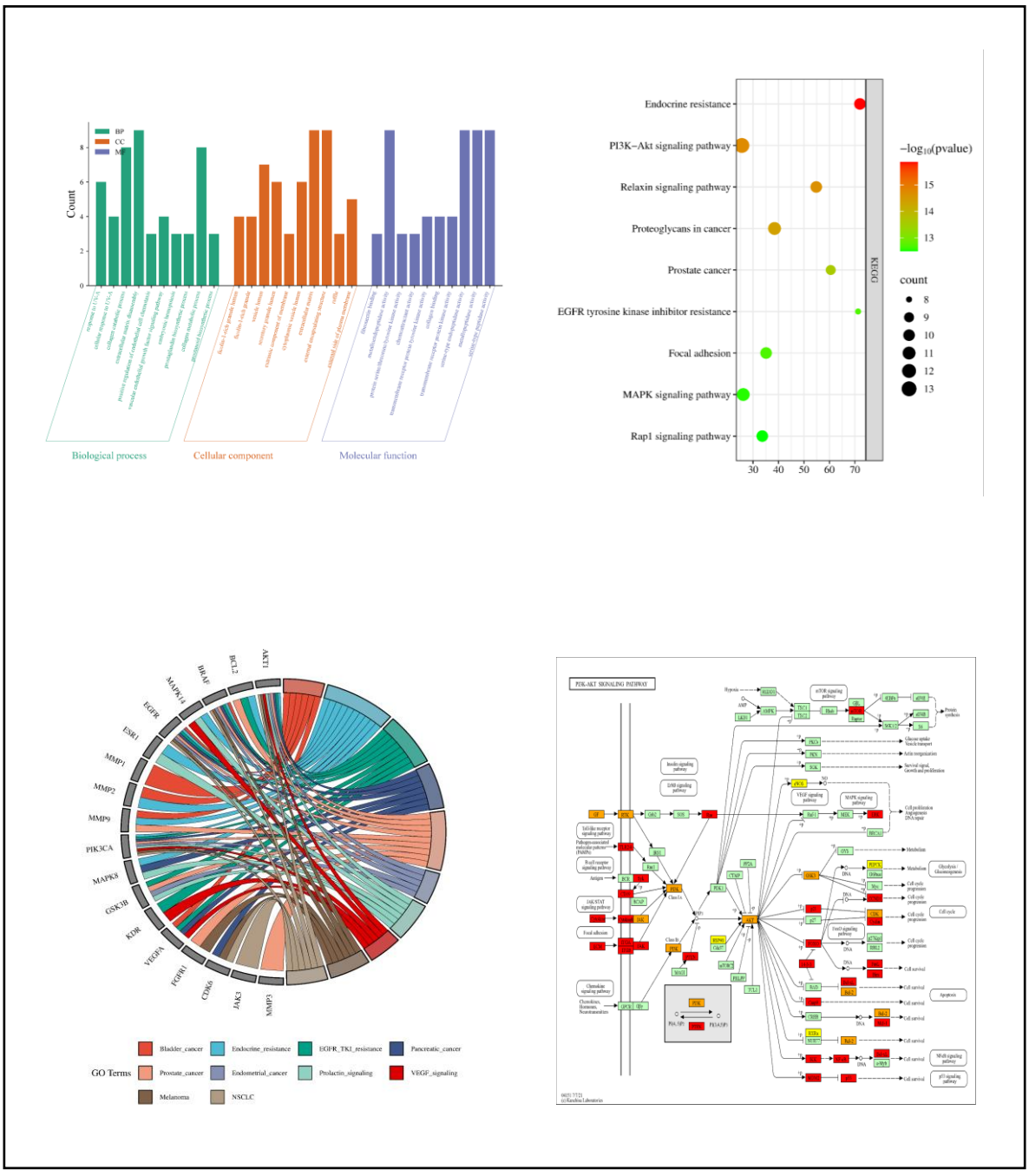


Figure 5. GO functional and KEGG pathway enrichment analyses of the identified targets. (A) GO enrichment analysis showing the Biological Process (BP), Cellular Component (CC), and Molecular Function (MF) categories. (B) Bubble diagram of KEGG pathway (C) Chord diagram illustrating the relationships between enriched KEGG pathways and their associated target genes. (D) The PI3K–Akt signaling pathway was visualized using the KEGG Mapper. Orange nodes represent epicatechin-associated RA targets, yellow nodes represent epicatechin-associated targets that do not overlap with RA-associated targets, and red nodes represent other RA-associated targets within the PI3K–Akt signaling pathway.

Drug–Compound-Target–Pathway-Disease (D-C-T-P-D) Network Construction

The D-C-T-P-D network of epicatechin for the treatment of rheumatoid arthritis comprised 56 total nodes (43 target genes, 10 core pathways, one epicatechin node, one Chaetomium globosum node, and one rheumatoid arthritis node) and 664 edges (Figure 6). The target genes, epicatechin and C. globosum, core pathways, and rheumatoid arthritis were represented by yellow, green, blue, and red nodes, respectively. The degree of epicatechin was 43. The PI3K–Akt signaling

pathway showed a degree of 14, whereas AKT1 showed a degree of 75, identifying AKT1 as the potential target associated with rheumatoid arthritis.

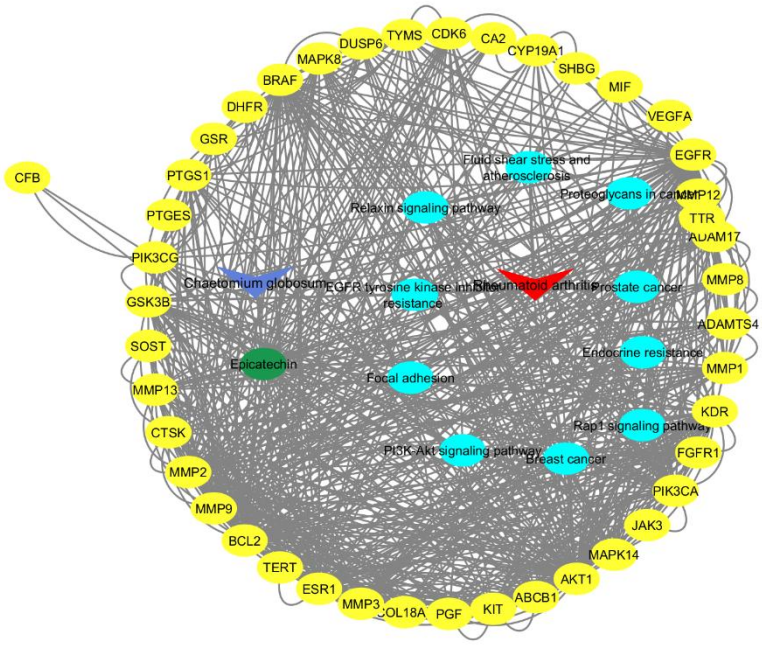
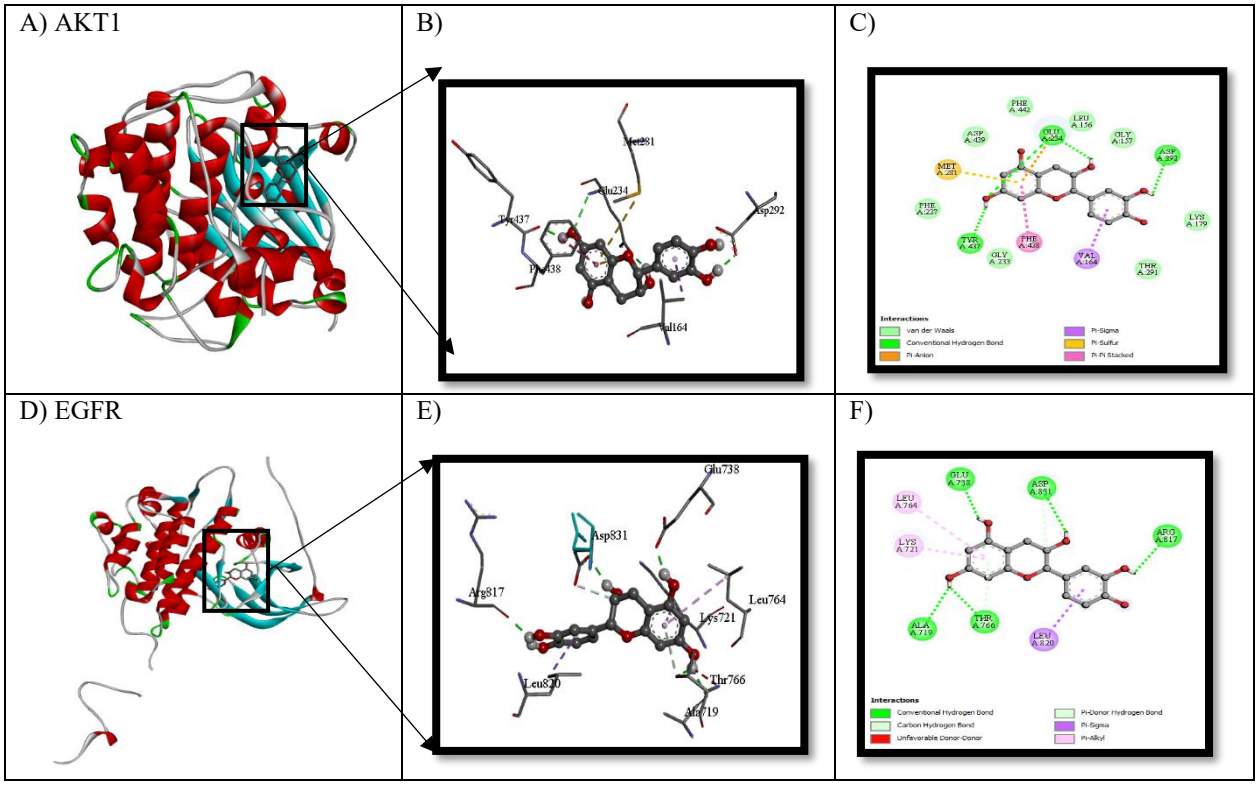


Fig 6. The drug-compound-target-pathway-disease network showed the mechanism of Epicatechin to treat RA.

Molecular docking

Molecular docking analysis showed that epicatechin interacted with all selected RA-associated targets, with predicted binding energies ranging from −4.18 to −9.57 kcal/mol. The most negative binding energy was observed for KDR (−9.57 kcal/mol), followed by MMP3 (−8.90 kcal/mol), AKT1 (−7.72 kcal/mol), EGFR (−7.46 kcal/mol), MMP9 (−5.63 kcal/mol) and BCL2 (−4.18 kcal/mol). The binding energies of epicatechin against the selected core targets is depicted as a heatmap in Figure 8. Epicatechin formed multiple hydrogen-bond and non-covalent interactions with key residues, including GLU234, ASP292 and TYR437 (AKT1); GLU738, ASP831 and ARG817 (EGFR); TYR927, ASN1040 and GLU1038 (KDR); GLU111, PHE110 and GLY186 (MMP9); ALA217, ALA165 and TYR223 (MMP3); and ASP168 and ALA30 (BCL2). KDR and MMP9 showed the highest number of conventional hydrogen bonds (five each). Amide–π stacked interactions were observed with ASP998 in KDR and HIS201 in MMP3. The docking poses and interaction profiles are shown in Figure 7.



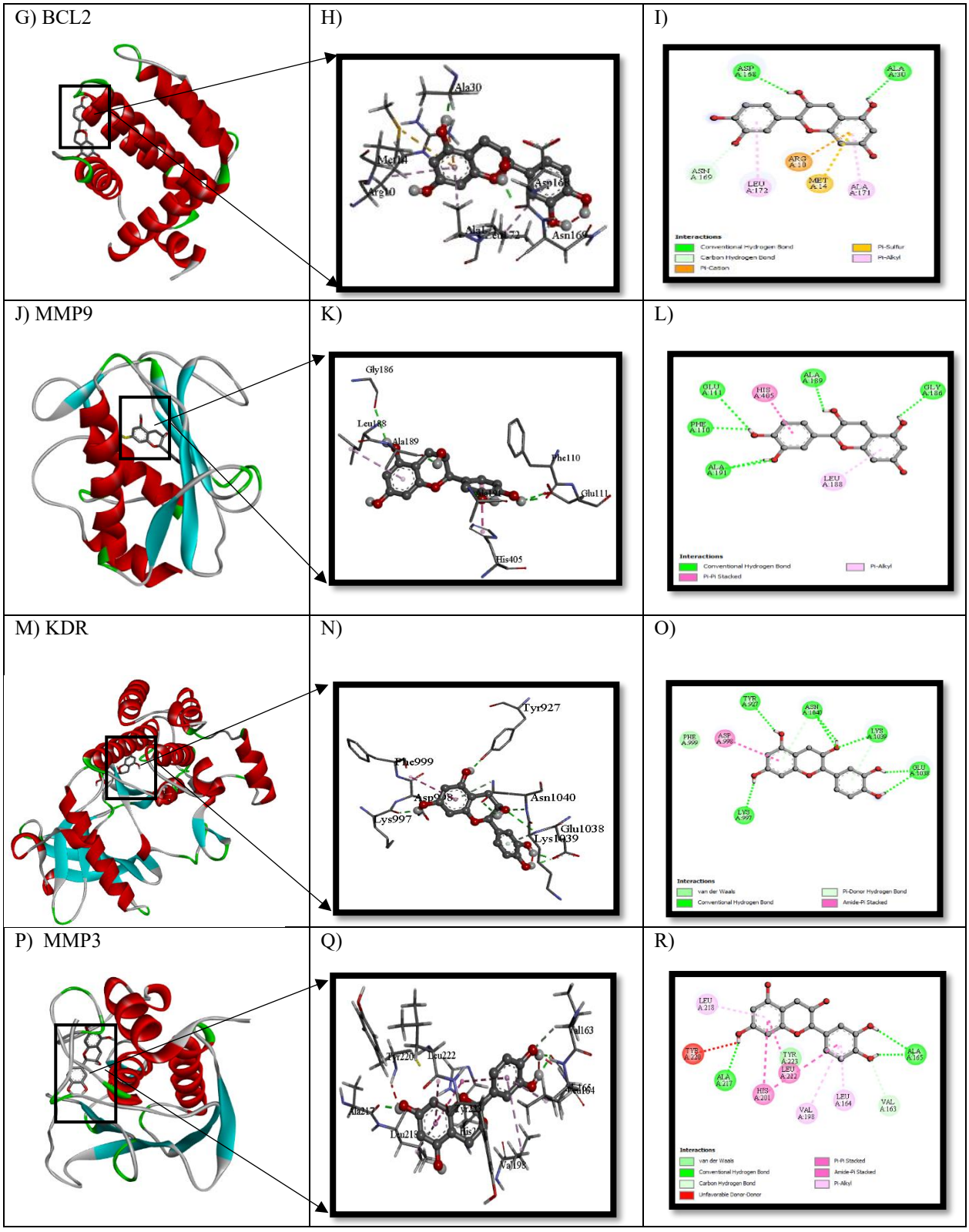


Figure 7. Molecular docking interactions of epicatechin with selected core targets of RA. . (A–C) AKT1; (D–F) EGFR; (G–I) BCL2; (J–L) MMP9; (M–O) KDR; and (P–R) MMP3. For each target, the panels show (A, D, G, J, M, P) the three-dimensional protein–epicatechin complex, (B, E, H, K, N, Q) the enlarged binding pose, and (C, F, I, L, O, R) the corresponding two-dimensional interaction profile showing the interacting amino-acid residues and non-covalent interactions.

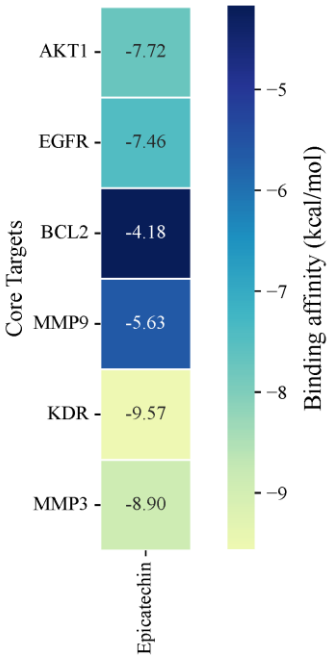


Fig. 8. Heatmap depicting the predicted binding energies of epicatechin with selected core targets of rheumatoid arthritis.

DISCUSSION

Rheumatoid arthritis (RA) is a chronic inflammatory disease characterized by persistent synovial inflammation and progressive joint tissue damage (Haque et al., 2021). Methotrexate and other disease-modifying antirheumatic drugs are widely used in RA treatment; however, treatment may require modification when adequate disease control is not achieved. Safety considerations also influence treatment selection, particularly minimizing glucocorticoid exposure and considering cardiovascular, malignancy and thromboembolic risk factors associated with JAK inhibition (Fraenkel et al., 2021; Smolen et al., 2023). Therefore, multi-target therapeutic strategies with lower toxicity and the ability to modulate multiple disease-associated pathways remain of considerable interest.

Endophytic fungi associated with medicinal plants have been investigated as sources of bioactive metabolites (Rai et al., 2021). Drynaria quercifolia (L.) J. Sm., traditionally used for rheumatic conditions, has demonstrated anti-inflammatory effects in experimental models of rheumatoid arthritis (Saravanan et al., 2013; Modak et al., 2021). In our previous study, Chaetomium globosum SK04 isolated from D. quercifolia demonstrated antioxidant and anti-inflammatory activities (Swetha et al., 2026). Similarly, a methanolic extract of C. globosum isolated from Adiantum capillus-veneris exhibited inhibitory effects in an adjuvant-induced arthritis model (Abdel-Azeem et al., 2016). However, the metabolites associated with the observed activities of SK04 extract remained insufficiently characterized. Therefore, the present study extended these observations by characterizing metabolites associated with the most active fraction of SK04 and exploring the potential interactions of the major compound with RA-associated targets using network pharmacology and molecular docking.

Among the fractions obtained from the ethyl acetate extract of C. globosum SK04, MF5 exhibited the highest anti-inflammatory activity and was therefore selected for metabolite characterization. LC–MS/MS profiling of MF5 identified eight metabolites with varying relative abundances, representing different chemical classes, including phenolic acids, a coumarin, an alkaloid, flavonoids, and a flavonoid glycoside. Such chemical diversity has also been reported among C. globosum isolates (Goda et al., 2023). Vanillic acid has been associated with antioxidant, anti-inflammatory, and antimicrobial activities, The presence of phenolic metabolites in MF5 is also consistent with previous reports on the host plant D. quercifolia, in which p-coumaric acid-O-hexoside was identified by UPLC–TQD–MS (Devanesan et al., 2025). This indicates that endophytic fungi can produce metabolites similar to those found in their host plants (Wen et al., 2022). Flavonoids detected in MF5 may also contribute to its anti-inflammatory activity, as kaempferol has been reported to exert anti-inflammatory effects in RA-FLS (Ling et al., 2024). Epicatechin was detected at m/z 289.0722 $[M–H]^-$, with product ions at m/z 245.1, 205.1, and 179.1, and the observed fragmentation pattern was consistent with previously reported catechin/epicatechin fragmentation (Lin et al., 2014). However, catechin and epicatechin are stereoisomers and therefore cannot be reliably distinguished solely by MS/MS analysis. The relevance of epicatechin to rheumatoid arthritis is supported by Fechtner et al. (2017), who investigated epicatechin and other catechins in IL-1β-stimulated RA synovial fibroblasts and reported effects on TAK1, an upstream regulator of inflammatory signalling. Based on its prominent chromatographic peak and reported effects on inflammatory signalling, epicatechin was selected for subsequent network pharmacology analysis to explore its potential targets and pathways associated with RA. Nevertheless, the contribution of other metabolites present at lower abundances to the overall biological activity of MF5 cannot be excluded.

Target prediction identified 126 non-redundant potential targets of epicatechin, of which 43 overlapped with genes involved in RA. Catechin, a structurally related flavan-3-ol, has also been reported in C. globosum, with anti-inflammatory activity through modulation of MAPK and NF-κB signalling pathways (Ningaraju et al., 2021). These findings provided a basis for further analysis of the predicted epicatechin targets in relation to RA-associated signalling pathways.

Persistent inflammatory stimulation alters the phenotype of RA-FLS, promoting cellular proliferation, migration and production of inflammatory mediators and matrix-degrading enzymes (Nygaard and Firestein, 2020; McInnes and Schett, 2011). The PPI network revealed extensive interactions among the shared targets, with AKT1, MMP9, BCL2, KDR, MMP3, MMP2, ESR1, EGFR, PIK3CA and BRAF occupying highly connected positions. These proteins are involved in intracellular signalling, cell survival, extracellular-matrix remodelling and angiogenesis related process in RA (Elshabrawy et al., 2015). AKT1 and PIK3CA were prominent components of the PI3K–AKT pathway, with AKT1 showing the highest connectivity. This finding is consistent with experimental evidence linking PI3K–AKT activation to pathological RA-FLS responses, while inhibition of this pathway reduces cellular proliferation, migration and inflammatory activity and AKT1 was also identified as a relevant molecular target in an experimental anti-RA mechanism (Yang et al., 2024; Gao et al., 2025). The central position of AKT1 within the network therefore indicates its potential relevance to the predicted epicatechin-associated molecular interactions.

The relationships between epicatechin, the shared targets and enriched pathways were further represented in the D-C-T-P-D network. Epicatechin was connected with multiple target proteins distributed across several RA-associated pathways, indicating a multi-target interaction pattern. The PI3K–AKT pathway was particularly prominent in the network. Several matrix metalloproteinases, including MMP1, MMP2, MMP3, MMP9 and MMP13, were also present among the predicted targets. Activated RA-FLS produce matrix metalloproteinases that contribute to extracellular-matrix degradation and joint tissue destruction (Nygaard and Firestein, 2020). EGFR-associated signalling has been linked to MMP9 regulation through the PI3K–AKT axis in experimental RA (Luo et al., 2025). The presence of EGFR, AKT1 and multiple MMPs in the predicted target network therefore connects intracellular signalling with extracellular-matrix remodelling. KDR/VEGFR2-mediated VEGF signalling is also involved in synovial angiogenesis and vascular remodelling, processes that contribute to the expansion of inflamed synovial tissue and recruitment of inflammatory cells (Zhao et al., 2025).

MAPK signalling was also enriched in the present analysis and is involved in inflammatory activation, proliferation and migration of RA synovial cells (Xie et al., 2025). Focal-adhesion signalling is associated with cell adhesion and cytoskeletal processes underlying fibroblast motility, and focal-adhesion-associated proteins have been implicated in the motility of arthritic fibroblast-like synoviocytes (Beckmann et al., 2024). The enrichment of PI3K–AKT, MAPK and focal-adhesion pathways therefore links the predicted targets with cellular processes involved in synovial activation and tissue remodelling. Other enriched pathways, including Rap1, relaxin and endocrine-resistance signalling, have also been associated with RA-related cellular and inflammatory processes (Kojima et al., 2009; Zhang et al., 2023; Wang et al., 2022).

Based on their network connectivity and biological relevance to RA-associated processes, AKT1, EGFR, BCL2, MMP9, KDR and MMP3 were selected as core targets for molecular docking analysis. Molecular docking analysis showed predicted interactions of epicatechin with these targets, with binding energies ranging from −4.18 to −9.57 kcal/mol. Among the selected targets, AKT1 occupied the most central position in the target network, whereas KDR showed the most negative binding energy (−9.57 kcal/mol). These findings suggest that epicatechin may interact with targets involved in signalling processes related to synovial-cell activation, migration and tissue remodelling in RA. Further experimental studies are needed to validate these predicted epicatechin–target interactions and determine their relevance to RA-associated signalling pathways.

CONCLUSION

The present study highlights the potential of Chaetomium globosum SK04 isolated from Drynaria quercifolia as a source of bioactive metabolites with anti-inflammatory activity. Epicatechin was identified as a major metabolite in the most active fraction, and its molecular analysis revealed interactions with multiple RA-associated targets, with AKT1 occupying a central position in the target network and PI3K–Akt signalling emerging as a prominent pathway. KDR showed the most favourable predicted binding among the core targets, indicating a strong predicted interaction with epicatechin. The integrated analysis provides insights into the molecular basis of epicatechin activity in rheumatoid arthritis. Further experimental studies are needed to determine the efficacy, safety, and therapeutic potential of epicatechin for rheumatoid arthritis.

REFERENCES

1. Abdel-Azeem, A. M., Zaki, S. M., Khalil, W. F., Makhlouf, N. A., & Farghaly, L. M. (2016). Anti-rheumatoid activity of secondary metabolites produced by endophytic Chaetomium globosum. Frontiers in Microbiology, 7, 1477. https://doi.org/10.3389/fmicb.2016.01477
2. Alam, B., Lǐ, J., Gě, Q., Khan, M. A., Gōng, J., Mehmood, S., ... & Gǒng, W. (2021). Endophytic fungi: from symbiosis to secondary metabolite communications or vice versa?..Frontiers in Plant Science, 12, 791033. https://doi.org/10.3389/fpls.2021.791033 Frontiers
3. Beckmann, D., Krause, A., Hansen, U., Kiener, H. P., Karonitsch, T., Blüml, S., Kremerskothen, J., Pavenstädt, H., Pap, T., & Korb-Pap, A. (2024). Focal adhesion protein Lasp1 links the Arp2/3 complex to adherens junctions and promotes motility of arthritic fibroblast-like synoviocytes. Annals of the Rheumatic Diseases, 83(6), 816–819. https://doi.org/10.1136/ard-2023-225241
4. Daina, A., & Zoete, V. (2024). Testing the predictive power of reverse screening to infer drug targets, with the help of machine learning. Communications Chemistry, 7, 105. https://doi.org/10.1038/s42004-024-01179-2
5. Devanesan, A. A., Garlapati, D., Abraham, S. V. P. I., Ameer, A. S., Gnanaselvan, S., Chandran, A., Veerapandian, R., Nandakumar, S., Rajamanickam, R., Vijayaraghavan, M., & Sundan, S. (2025). Biological activity of Drynaria quercifolia (Polypodiaceae) rhizome extract phytocompounds against A549 lung cancer cells: A molecular docking study. Plant Biosystems, 159(4), 668–681. https://doi.org/10.1080/11263504.2025.2496477

6. Ding, Q., Hu, W., Wang, R., Yang, Q., Zhu, M., Li, M., Cai, J., Rose, P., Mao, J., & Zhu, Y. Z. (2023). Signaling pathways in rheumatoid arthritis: Implications for targeted therapy. Signal Transduction and Targeted Therapy, 8(1), 68. https://doi.org/10.1038/s41392-023-01331-9 Nature
7. Elshabrawy, H. A., Chen, Z., Volin, M. V., Ravella, S., Virupannavar, S., & Shahrara, S. (2015). The pathogenic role of angiogenesis in rheumatoid arthritis. Angiogenesis, 18(4), 433–448. https://doi.org/10.1007/s10456-015-9477-2
8. Fechtner, S., Singh, A., Chourasia, M., & Ahmed, S. (2017). Molecular insights into the differences in anti-inflammatory activities of green tea catechins on IL-1β signaling in rheumatoid arthritis synovial fibroblasts. Toxicology and Applied Pharmacology, 329, 112–120. https://doi.org/10.1016/j.taap.2017.05.016
9. Fraenkel, L., Bathon, J. M., England, B. R., St. Clair, E. W., Arayssi, T., Carandang, K., ... & Akl, E. A. (2021). 2021 American College of Rheumatology guideline for the treatment of rheumatoid arthritis. Arthritis & Rheumatology, 73(7), 1108–1123. https://doi.org/10.1002/art.41752
10. Gao, C., Song, X.-D., Chen, F.-H., Wei, G.-L., & Guo, C.-Y. (2024). The protective effect of natural medicines in rheumatoid arthritis via inhibit angiogenesis. Frontiers in Pharmacology, 15, 1380098. https://doi.org/10.3389/fphar.2024.1380098
11. Gao, X., Lyu, S., Lin, T., He, J., Pan, W., He, J., Wang, X., Lin, X., Chen, J., & Wang, Q. (2025). Oxyimperatorin suppresses the pathologies of rheumatoid arthritis and the growth of synovial organoids through targeting the PI3K/AKT pathway. Phytotherapy Research, 39(8), 3526–3544. https://doi.org/10.1002/ptr.70009
12. Goda, M. S., El-Kattan, N., Abdel-Azeem, M. A., Allam, K. A. M., Badr, J. M., Nassar, N. A., Almalki, A. J., Alharbi, M., Elhady, S. S., & Eltamany, E. E. (2023). Antimicrobial potential of different isolates of Chaetomium globosum combined with liquid chromatography tandem mass spectrometry chemical profiling. Biomolecules, 13(12), 1683. https://doi.org/10.3390/biom13121683
13. Haque, M., Singh, A. K., Ouseph, M. M., & Ahmed, S. (2021). Regulation of synovial inflammation and tissue destruction by guanylate binding protein 5 in synovial fibroblasts from patients with rheumatoid arthritis and rats with adjuvant-induced arthritis. Arthritis & Rheumatology, 73(6), 943–954. https://doi.org/10.1002/art.41611
14. Harlianto, N. I., & GBD 2021 Rheumatoid Arthritis Collaborators. (2023). Global, regional, and national burden of rheumatoid arthritis, 1990–2020, and projections to 2050: A systematic analysis of the Global Burden of Disease Study 2021. The Lancet Rheumatology, 5(10), e594–e610. https://doi.org/10.1016/S2665-9913(23)00211-4
15. Jegan, G., Kaavya, A., Keerthana, E., & Sneha, S. (2025). Phytochemical screening and anti inflammatory activity of Drynaria quercifolia rhizome. Biosciences, Biotechnology Research Asia, 22(1), 359. https://doi.org/10.13005/bbra/3367 Biotech Asia
16. Kojima, F., Kapoor, M., Kawai, S., Yang, L., Aronoff, D. M., & Crofford, L. J. (2009). Prostaglandin E2 activates Rap1 via EP2/EP4 receptors and cAMP-signaling in rheumatoid synovial fibroblasts: Involvement of Epac1 and PKA. Prostaglandins & Other Lipid Mediators, 89(1–2), 26–33. https://doi.org/10.1016/j.prostaglandins.2009.03.001
17. Komatsu, N., & Takayanagi, H. (2022). Mechanisms of joint destruction in rheumatoid arthritis—immune cell–fibroblast–bone interactions. Nature Reviews Rheumatology, 18(7), 415–429. https://doi.org/10.1038/s41584-022-00793-5 Nature
18. Kumar Gandham, S., Jha, A., & Kudale, A. A. (2024). Design and Synthesis of 2-Phenylindolizine Acetamides: Molecular Docking, in Vitro Antimicrobial and Anticancer Activity Evaluation. Chemistry & Biodiversity, 21(5), e202400075. https://doi.org/10.1002/cbdv.202400075
19. Li, J., Zhang, X., Guo, D., Shi, Y., Zhang, S., Yang, R., & Cheng, J. (2023). The mechanism of action of paeoniae radix rubra–angelicae sinensis radix drug pair in the treatment of rheumatoid arthritis through PI3K/AKT/NF-κB signaling pathway. Frontiers in Pharmacology, 14, 1113810. https://doi.org/10.3389/fphar.2023.1113810
20. Lin, L.-Z., Sun, J., Chen, P., Monagas, M. J., & Harnly, J. M. (2014). UHPLC-PDA-ESI/HRMSn profiling method to identify and quantify oligomeric proanthocyanidins in plant products. Journal of Agricultural and Food Chemistry, 62(39), 9387. https://doi.org/10.1021/jf501011y
21. Ling, Y., Ren, N., Yang, Y., Xu, H., Xiong, H., Wang, Q., Lu, D., Yao, X., & Ma, W. (2024). Kaempferol alleviates rheumatoid arthritis through pyroptosis based on bioinformatics analysis and experimental validation. Scientific Reports, 14, 29769. https://doi.org/10.1038/s41598-024-81833-w
22. Liu, X., Ouyang, S., Yu, B., Liu, Y., Huang, K., Gong, J., Zheng, S., Li, Z., Li, H., & Jiang, H. (2010). PharmMapper server: A web server for potential drug target identification using pharmacophore mapping approach. Nucleic Acids Research, 38(Suppl. 2), W609–W614. https://doi.org/10.1093/nar/gkq300
23. Luo, J.-F., Yu, Y., & Liu, J.-X. (2025). Mechanism of asperosaponin VI related to EGFR/MMP9/AKT/PI3K pathway in treatment of rheumatoid arthritis. Chinese Journal of Integrative Medicine, 31(2), 131–141. https://doi.org/10.1007/s11655-024-3767-8
24. McInnes, I. B., & Schett, G. (2011). The pathogenesis of rheumatoid arthritis. New England Journal of Medicine, 365(23), 2205–2219. https://doi.org/10.1056/NEJMra1004965
25. Modak, D., Ghosh, S., Sarkar, S., Roy, S. K., Chakraborty, A., Ray, A., Patel, C. N., Georrge, J. J., Thakur, S., & Bhattacharjee, S. (2025). Unveiling the mechanism of amelioration of adjuvant-induced rheumatoid arthritis by Drynaria quercifolia rhizome extract using network pharmacology and gene expression-based studies. Scientific Reports, 15(1), 11981. https://doi.org/10.1038/s41598-025-87461-2
26. Modak, D., Paul, S., Sarkar, S., Thakur, S., & Bhattacharjee, S. (2021). Validating potent anti-inflammatory and anti-rheumatoid properties of Drynaria quercifolia rhizome methanolic extract through in vitro, in vivo, in silico and GC-MS-based profiling. BMC Complementary Medicine and Therapies, 21 (1), 89. https://doi.org/10.1186/s12906-021-03265-7

27. Ningaraju, S., Munawer, U., Raghavendra, V. B., Balaji, K. S., Melappa, G., Brindhadevi, K., & Pugazhendhi, A. (2021). Chaetomium globosum extract mediated gold nanoparticle synthesis and potent anti-inflammatory activity. Analytical Biochemistry, 612, 113970. https://doi.org/10.1016/j.ab.2020.113970
28. Nygaard, G., & Firestein, G. S. (2020). Restoring synovial homeostasis in rheumatoid arthritis by targeting fibroblast-like synoviocytes. Nature Reviews Rheumatology, 16(6), 316–333. https://doi.org/10.1038/s41584-020-0413-5
29. Padyukov, L. (2022). Genetics of rheumatoid arthritis. Seminars in Immunopathology, 44(1), 47–62. https://doi.org/10.1007/s00281-022-00912-0 PubMed Central (PMC)
30. Piñero, J., Saüch, J., Sanz, F., & Furlong, L. I. (2021). The DisGeNET Cytoscape app: Exploring and visualizing disease genomics data. https://doi.org/10.1016/j.csbj.2021.05.015
31. Rai, N., Keshri, P. K., Verma, A., & Kamble, S. C. (2021). Plant associated fungal endophytes as a source of natural bioactive compounds. Mycology, 12(3), 139–159. https://doi.org/10.1080/21501203.2020.1870579
32. Saravanan, S., Mutheeswaran, S., Saravanan, M., Chellappandian, M., Gabriel Paulraj, M., Karunai Raj, M., Ignacimuthu, S., & Duraipandiyan, V. (2013). Ameliorative effect of Drynaria quercifolia (L.) J. Sm., an ethnomedicinal plant, in arthritic animals. Food and Chemical Toxicology, 51, 356–363. https://doi.org/10.1016/j.fct.2012.10.020
33. Smolen, J. S., Landewé, R. B. M., Bergstra, S. A., Kerschbaumer, A., Sepriano, A., Aletaha, D., Caporali, R., Edwards, C. J., Hyrich, K. L., Pope, J. E., de Wit, M., & Baraliakos, X. (2023). EULAR recommendations for the management of rheumatoid arthritis with synthetic and biological disease-modifying antirheumatic drugs: 2022 update. Annals of the Rheumatic Diseases, 82(1), 3–18. https://doi.org/10.1136/ard-2022-223356
34. Swetha, R., Viswanathan, S., Pushpalingam, K., & Kirthiga, B. (2026). Anti-inflammatory potential of endophytic Chaetomium globosum from Drynaria quercifolia: In vitro evaluation and in silico investigation of NFκB signalling modulation. International Journal of Drug Delivery Technology, 16(70s), 667–687. https://doi.org/10.25258/ijddt.16.70s.69
35. Szklarczyk, D., Kirsch, R., Koutrouli, M., Nastou, K., Mehryary, F., Hachilif, R., Gable, A. L., Fang, T., Doncheva, N. T., Pyysalo, S., Bork, P., & Jensen, L. J. (2023). The STRING database in 2023: Protein–protein association networks and functional enrichment analyses for any sequenced genome of interest. Nucleic Acids Research, 51(D1), D638–D646. https://doi.org/10.1093/nar/gkac1000
36. Wang, Q., Yao, X., Ling, Y., Huang, Y., Chen, C., Hou, L., Yang, Y., Wu, H., & Ma, W. (2022). Investigation of the mechanism of Periploca forrestii against rheumatoid arthritis with network pharmacology-based analysis. Evidence-Based Complementary and Alternative Medicine, 2022 (1), 2993374. https://doi.org/10.1155/2022/2993374
37. Wen, J., Okyere, S. K., Wang, S., Wang, J., Xie, L., Ran, Y., & Hu, Y. (2022). Endophytic fungi: An effective alternative source of plant-derived bioactive compounds for pharmacological studies. Journal of Fungi, 8(2), 205. https://doi.org/10.3390/jof8020205
38. Xie, J., Sun, S., Li, Q., Chen, Y., Huang, L., Wang, D., & Wang, Y. (2025). MAPK/ERK signaling pathway in rheumatoid arthritis: Mechanisms and therapeutic potential. PeerJ, 13, e19708. https://doi.org/10.7717/peerj.19708
39. Yang, H., Liu, C., Lin, X., Li, X., Zeng, S., Gong, Z., Xu, Q., Li, D., & Li, N. (2024). Wogonin inhibits the migration and invasion of fibroblast-like synoviocytes by targeting PI3K/AKT/NF-κB pathway in rheumatoid arthritis. Archives of Biochemistry and Biophysics, 755, 109965. https://doi.org/10.1016/j.abb.2024.109965
40. Zhang, M., Vervoort, L., Moalin, M., Mommers, A., Douny, C., den Hartog, G. J. M., & Haenen, G. R. M. (2018). The chemical reactivity of (−)-epicatechin quinone mainly resides in its B-ring. Free Radical Biology and Medicine, 124, 31–39. https://doi.org/10.1016/j.freeradbiomed.2018.05.087
41. Zhao, F., Hu, Z., Li, G., Liu, M., Huang, Q., Ai, K., & Cai, X. (2025). Angiogenesis in rheumatoid arthritis: Pathological characterization, pathogenic mechanisms, and nano-targeted therapeutic strategies. Bioactive Materials, 50, 603–639. https://doi.org/10.1016/j.bioactmat.2025.04.026
42. Zhou, Y., Zhou, B., Pache, L., Chang, M., Khodabakhshi, A. H., Tanaseichuk, O., Benner, C., & Chanda, S. K. (2019). Metascape provides a biologist-oriented resource for the analysis of systems-level datasets. Nature Communications, 10(1), 1523. https://doi.org/10.1038/s41467-019-09234-6